Hadronic Final States and Parton Density Functions

H. Jung

Abstract: A program to determine the unintegrated parton density functions from hadronic final state and inclusive measurements, including diffraction, is outlined. As a by-product the integrated pdfs are determined and α_s can be measured in a different approach.

1 Introduction

The idea presented here is to focus on the experimental determination of parton density functions. Whereas in HERA 1 $F_2(x, Q^2)$ was the source for constraining the proton parton density functions (PDF's), the high statistics data of HERA 2 offer the possibility to further constrain the PDF's with hadronic final state measurements in addition to $F_2(x, Q^2)$. Hadronic final states can be either jet measurements and/or whole area of heavy flavor production, including also diffraction.

Combining final state measurements with inclusive measurements not only further constrains the PDF's, but also allows the determination of unintegrated (x, $k_\perp$, μ dependent) PDF's (uPDF), which can only be done at HERA and which will become more and more important for physics at the LHC. The uPDF's can be either in the DGLAP type, or with the small x improved descriptions. They are also best suited to make the connection to diffraction, the so-called dipole model and at the end also saturation. In addition, as a sort of by-product, the determination of α_s becomes also possible.

With the deep knowledge of the tracking detectors and triggers, the experience in hadronic final state and heavy quark analysis, and the knowledge of Monte Carlo generators and QCD evolution, the FH1 group is best suited to perform such a program. Performing different types of final state measurements together with a determination of the PDF's and the proper error analysis within one single group, provides besides a common goal also requires close communication and interaction within the group. At the end such a program could lead to a close collaboration with theory and phenomenology centers like Durham, Lund and Cracow, and eventually could create a QCD phenomenology center, including these groups, at DESY, which will strengthen the role of DESY if participating in LHC but also serves as a basic for a future linear collider project.

2 QCD factorization theorem

At high energies, even for small values of coupling constant α_s, the phase space for parton emissions increases fast, and therefore it is not sufficient to include only a few calculable terms in the perturbative expansion. This problem can be treated by resumming the leading logarithmic behavior of the cross section. The most important contribution at small x is gluon bremsstrahlung, with the typical behavior of being largest in the infrared and/or collinear region. Two different resummation strategies have been developed: the DGLAP [1–4] approach, resumming leading logarithms of ratios of subsequent virtualities also called collinear approach, and the BFKL [5–7] approach, resumming the infrared contributions, also called the $k_\perp$-factorization [8,9] or the semi-hard approach [10,11]. The CCFM [12–15] approach attempts to cover both the collinear and the infrared regions by considering color coherence effects, and in the limit of asymptotic energies is almost equivalent [16–18] to the BFKL and DGLAP evolution equations.

In the collinear approach the cross section is factorized into a process dependent hard scattering matrix element convoluted with universal parton density functions. Since strong ordering in virtualities is required in the evolution, the largest virtuality is in the hard scattering and therefore the virtuality of the partons entering the hard scattering matrix element can be neglected and they can be treated as being collinear with the incoming hadron[1]. Any physics process in the fixed order collinear factorization scheme is then calculated by a convolution of a process dependent coefficient function $C^a(\frac{x}{z})$ with collinear (independent of $k_\perp$) parton density functions at a scale μ_f^2 (e.g. $\mu_f^2 = Q^2$ in $F_2(x, Q^2)$ in deep inelastic scattering (DIS)):

$$\sigma = \sigma_0 \int \frac{dz}{z} C^a(\frac{x}{z}) f_a(z,\, \mu_f^2) \tag{1}$$

As is usual in the collinear formulation of factorization, the coefficient functions are on-shell partonic cross sections with subtractions of the singular collinear regions. The parton distributions are typically in the $\overline{\rm MS}$ scheme, where the partons are integrated over *all* transverse momentum with the resulting ultraviolet divergences being canceled by renormalization in the $\overline{\rm MS}$ scheme. There is an evident mismatch of approximated and exact parton kinematics in such calculations. For the so-called *infra-red-safe* jet cross sections which are the domain of validity of these calculations, the factorization theorem ensures that the calculations are consistent and valid.

While the DGLAP approach with fixed order coefficient- and splitting functions is phenomenologically successful for inclusive quantities like the structure

[1]However neglecting the transverse momentum of the partons even in the collinear approach has been criticized in Ref. [19] as being unnecessary and unphysical.

function $F_2(x, Q^2)$ in DIS, it is not fully satisfactory from a theoretical point of view, because *"the truncation of the splitting functions at a fixed perturbative order is equivalent to assuming that the dominant dynamical mechanism leading to scaling violations is the evolution of parton cascades with strongly ordered transverse momenta"* as Catani argued in Ref. [20].

In the $k_\perp$-factorization approach, the partons along the parton ladder are no longer ordered in transverse momentum. At large energies (small x) the evolution of parton densities proceeds over a large region in rapidity $\Delta y \sim \log(1/x)$ and effects of finite transverse momenta of the partons may become increasingly important. Cross sections can then be $k_\perp$ - factorized [10,11,8,9] into an off mass-shell ($k_\perp$ dependent) partonic cross section $\hat{\sigma}(\frac{x}{z}, k_\perp)$ and a $k_\perp$ - unintegrated parton density function $\mathcal{F}(z, k_\perp)$:

$$\sigma = \int \frac{dz}{z} d^2k_\perp \hat{\sigma}(\frac{x}{z}, k_\perp)\mathcal{F}(z, k_\perp) \tag{2}$$

The unintegrated gluon density $\mathcal{F}(z, k_\perp)$ is described by the BFKL evolution equation in the region of asymptotically large energies (small x).

An appropriate description valid for both, small and large x, is given by the CCFM evolution equation, resulting in an unintegrated gluon density $\mathcal{A}(x, k_\perp, \bar{q})$, which is a function also of the additional evolution scale $\bar{q}$ described below. This scale $\bar{q}$ is connected to the factorization scale μ_f in the collinear approach.

The transverse momenta of the partons entering the hard scattering can be seen as being generated by two sources: the intrinsic (primordial) transverse momentum, which reflects the Fermi motion of the partons in the hadron, typically of the order of one GeV, and the transverse momentum generated by the QCD evolution (DGLAP or BFKL/CCFM/LDC), which can reach large values, even in DGLAP up to the factorization scale. To disentangle both contributions the unintegrated pdf formulation is best suited, as will be discussed below. For exclusive components of the cross section, it is therefore better to use suitably defined unintegrated distributions and off-shell parton kinematics. For one treatment along these lines that is specifically designed to treat NLO corrections in the context of showering Monte-Carlo event generators, see the paper of Collins and Zu [19].

From the above it is clear, that parton density functions are much more than just the quark and gluon distributions obtained from fits to the structure function $F_2(x, Q^2)$. To obtain the best description of the measurements, un-integrated parton density functions need to be used, even for the collinear DGLAP approach, where the following relation holds:

$$xg(x, \mu^2) = \int_0^{\mu^2} dk_\perp^2 x\mathcal{G}(x, k_\perp^2) \tag{3}$$

with $xg(x,\mu^2)$ being any of the parameterizations of the standard collinear parton densities, and $x\mathcal{G}(x,k_\perp^2)$ being the DGLAP unintegrated parton density.

Applying $k_\perp$factorization with BFKL or CCFM parton evolution, different unintegrated parton densities are obtained, for example the CCFM unintegrated gluon density $x\mathcal{A}(x,k_\perp^2,\bar{q}^2)$, which depends also on the factorization scale $\bar{q}$.

Thus measuring in detail the unintegrated parton distribution function, much can be learned about the factorization approaches (collinear versus $k_\perp$factorization) and the parton evolution (DGLAP versus BFKL/CCFM).

One example showing the importance of unintegrated parton density function is Higgs production at high energies, which proceeds predominantly via gluon - gluon scattering. Much effort has been put into the calculation of higher order corrections in the collinear approach, not only for the calculation of the total production cross section, but also for the calculation of the transverse momentum spectrum of the Higgs boson [21–23]. At the large Tevatron or LHC energies and with an expected Higgs mass of $\mathcal{O}(100-200)$ GeV, the $k_\perp$-factorization approach can be also used to calculate the cross section, since the longitudinal momenta reach values of the same order as the average transverse momenta ($\sim$ 10(18) GeV for Tevatron (LHC) energies, respectively). Such calculations have been performed in [24] where it was noted that the different set of unintegrated gluon densities predict similar cross sections as a function of $p_\perp$ for Tevatron energies whereas at LHC the cross section differs by factors up to 3. This again clearly indicates the sensitivity to the details of the unintegrated gluon density, which can be determined much more precisely with the forthcoming measurements at HERA. Similar results have been obtained in Ref. [25,26], approximating the matrix element and the CCFM unintegrated gluon distribution and also applying doubly unintegrated parton distributions in Ref. [27].

3 Unintegrated Parton density functions

As $F_2(x,Q^2)$ is the most important source of constraining the integrated (collinear) parton density functions, which can only precisely measured at present at HERA, the hadronic finals states at HERA, jets or heavy flavors, are the only sources to constrain further the unintegrated parton density functions (uPDF), in addition to $F_2(x,Q^2)$.

The unintegrated gluon density can be written [15,28–30] in form of an integral equation:

$$\mathcal{A}(x,k_\perp,\bar{q}) = \mathcal{A}_0(x,k_\perp,\bar{q}) + \int \frac{dz}{z} \int \frac{d^2q}{\pi q^2} \Theta(\bar{q}-zq)\Delta_s(\bar{q},zq)\tilde{P}(z,q,k_\perp)\mathcal{A}\left(\frac{x}{z},k_t',q\right) \tag{4}$$

ith $k_t' = |\vec{k}_t + (1-z)\vec{q}|$ and with $\bar{q}$ being the factorization (evolution) scale: $\bar{q} > z_n q_n$, $q_n > z_{n-1} q_{n-1}$, ..., $q_1 > Q_0$ (angular ordering). Here q is used as a shorthand notation for the 2-dimensional vector of the rescaled transverse momentum $\vec{q} \equiv \vec{q}_t = \vec{p}_t/(1-z)$. The splitting function is given by $\tilde{P}(z, q, k_\perp)$. The Sudakov form factor $\Delta_s(q_2, q_1)$ gives the probability for having no radiation between q_1 and q_2:

$$\Delta_s(q_i, z_i q_{i-1}) = \exp\left(-\int_{(z_{i-1}q_{i-1})^2}^{q_i^2} \frac{dq^2}{q^2} \int_0^{1-Q_0/q} dz \frac{\bar{\alpha}_s(q^2(1-z)^2)}{1-z}\right) \qquad (5)$$

with $\bar{\alpha}_s = \frac{C_A \alpha_s}{\pi} = \frac{3\alpha_s}{\pi}$.

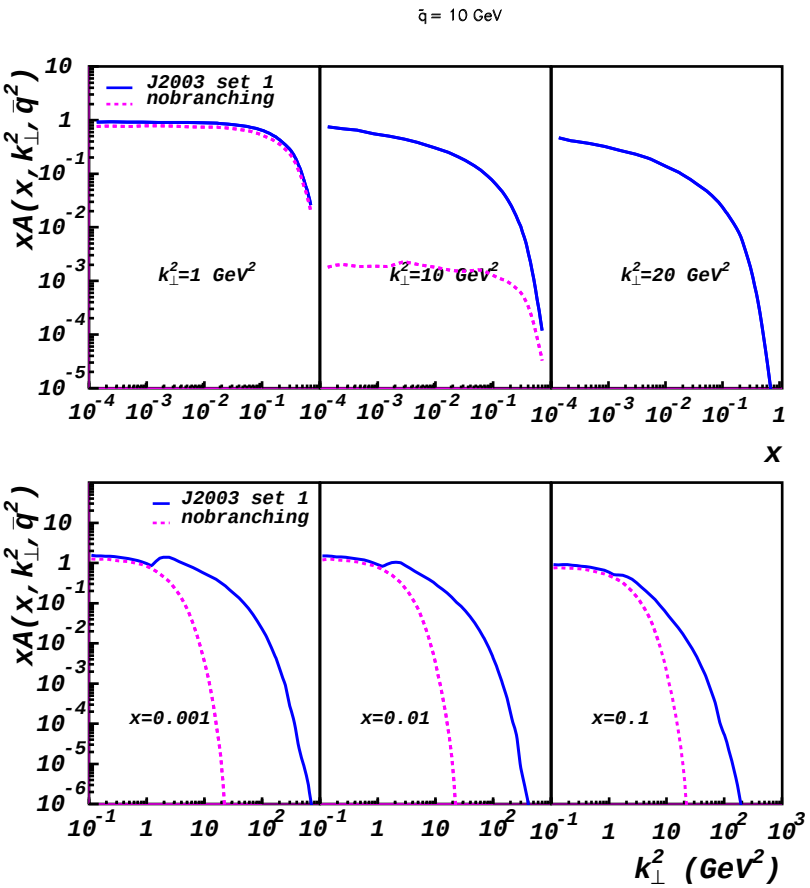

Figure 1: *Unintegrated CCFM gluon density as a function of x for different values of $k_\perp$ at $\bar{q} = 10$ GeV. Shown is the no-branching contribution of eq.(6) separately.*

The first term in the rhs of eq.(4) gives the probability for no-radiation from the starting scale Q_0 to the upper scale $\bar{q}$ and is given by:

$$\mathcal{A}_0(x, k_\perp, \bar{q}) = \mathcal{A}_0(x, k_\perp, Q_0) \cdot \Delta_s(\bar{q}, Q_0) \qquad (6)$$

and the second term in the rhs of eq.(4) describes the details of radiation. In Fig. 1 the different parts of eq.(4) are indicated for a CCFM uPDF.

3.0.1 Initial parton distribution: intrinsic $k_\perp$

The no-branching probability is directly sensitive to the initial (starting) distribution $\mathcal{A}_0(x, k_\perp, Q_0)$, and especially to the intrinsic $k_\perp$ distribution. The initial distribution of the $k_\perp$ unintegrated gluon distribution can be written as:

$$x\mathcal{A}_0(x, k_{t0}^2) = N \cdot 5\frac{1}{k_0^2}(1-x)^4 \cdot \exp\left(-k_{t0}^2/Q_s^2\right) \tag{7}$$

with Q_s^2 being a free parameter. In Fig. 2 the unintegrated gluon density is

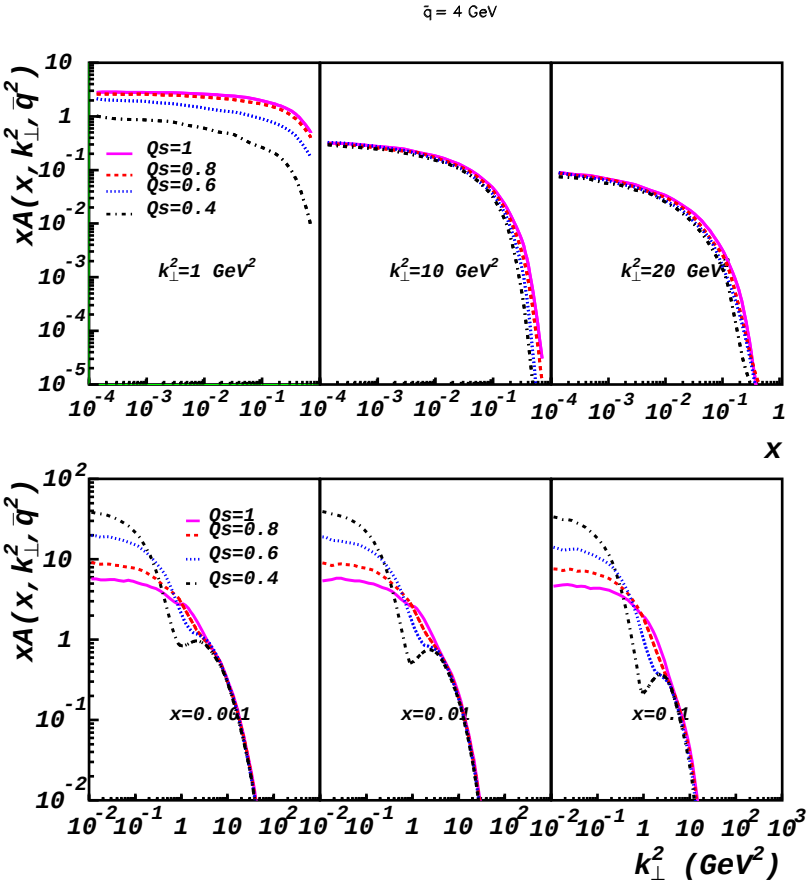

Figure 2: *Unintegrated CCFM gluon density as a function of x for different values of $k_\perp$ at $\bar{q} = 4$ GeV. Different choices for Q_s are shown.*

shown for different choices of Q_s. All the distributions displayed are fitted such that after convolution with the off-shell matrix element the inclusive structure function $F_2(x, Q^2)$ can be described with the same precision. On can observe huge differences (up to factors of 8) in the small $k_\perp$ region, whereas the large $k_\perp$ region is not much affected. This however allows for a experimental determination of the uPDF and to pin down the intrinsic parton distribution. In Fig. 3 the integrated gluon density obtained, from the uPDFs shown in Fig. 2, by integration over $k_\perp$ is shown. The effect of the different choices of Q_s are no longer visible as expected since they all are able to describe the structure function $F_2(x, Q^2)$. This shows clearly the advantage of using uPDFs: The information about the initial parton distribution can be clearly investigated and separated.

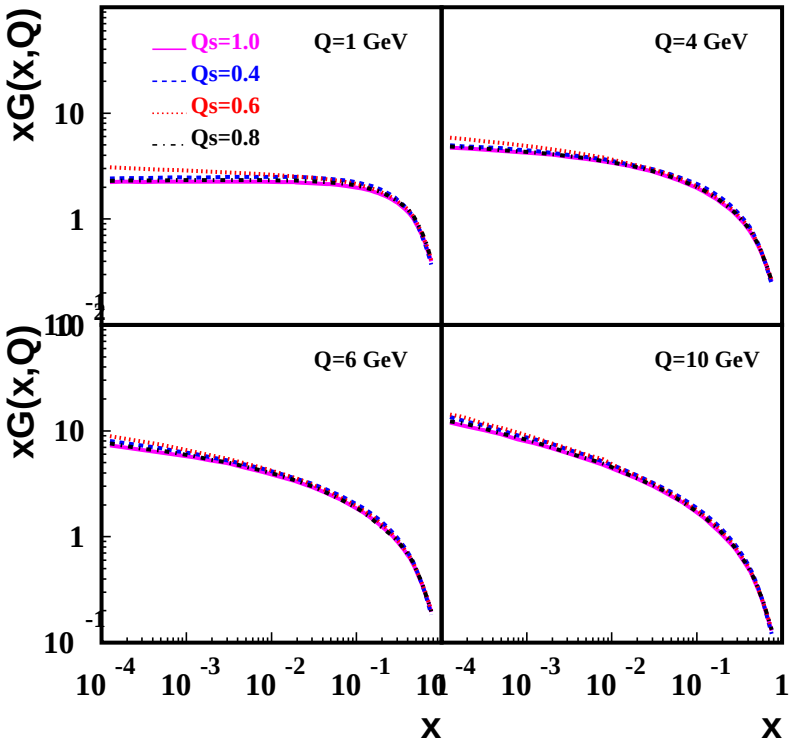

Figure 3: *Integrated gluon density for different values of the factorization scale* $\bar{q} = Q$. *The curves correspond to different values of* Q_s.

3.0.2 Saturation

It is believed that saturation occurs at rather low scales of order of $Q_s \sim 1$ GeV, the saturation scale of the GBW model is shown in Fig. 4 as a function of x:

$$Q_s(x) = \left(\frac{x}{x_0}\right)^{-\frac{\lambda}{2}} \tag{8}$$

with $x_0 = 0.00004$ and $\lambda = 0.28$. In Fig. 4 Q_s is shown for different values of x_0, showing that in the HERA range $Q_s < 1 - 2$ GeV. As shown above, the small $k_\perp$

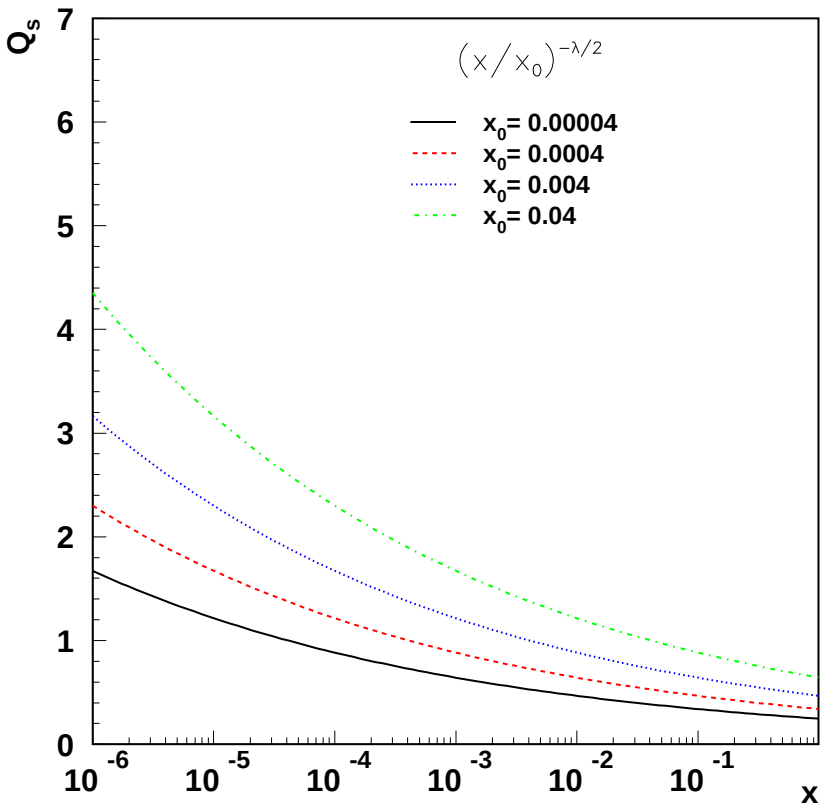

Figure 4: *The saturation scale Q_s as a function of x as obtaind by the Golec-Biernat Wusthoff model.*

region of the unintegrated pdf is highly sensitive to the intrinsic $k_\perp$ distribution. In Fig. 5 the unitegrated gluon distribution is shown using the GBW model as the starting distribution. A measurement of the unintegrated gluon distribution at small $k_\perp$ could clearly separate between the intrinisc $k_\perp$ distributions and the one obtained from the GBW model.

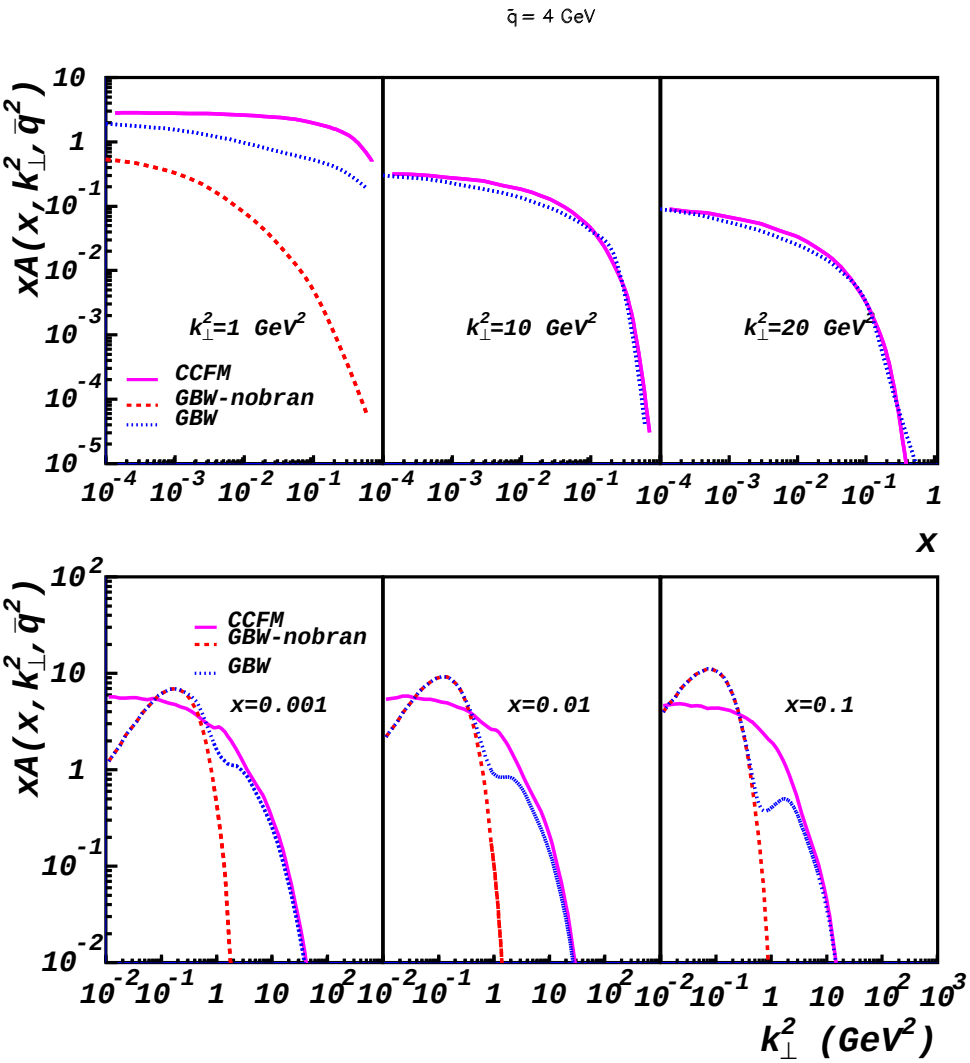

Figure 5: *Unintegrated CCFM gluon density as a function of x for different values of $k_\perp$ at $\bar{q} = 4$ GeV. The starting distribution is taken from the GBW model.*

However, also during the evolution in a non-$k_\perp$-ordered ladder, the small $k_\perp \leq Q_s$ region can be reached. If $Q_s > 1$ GeV the region of perturbative saturation effects is reached. To illustrate this effect, the saturation scale Q_s was used as an effective $k_\perp$-cut in the CCFM evoultion, below which no further radiation is obtained. This is a poor-man's approach to saturation. The effect is visualized in Fig. 6, for different values of x_0 and the corresponding different values of the saturation scale Q_s.

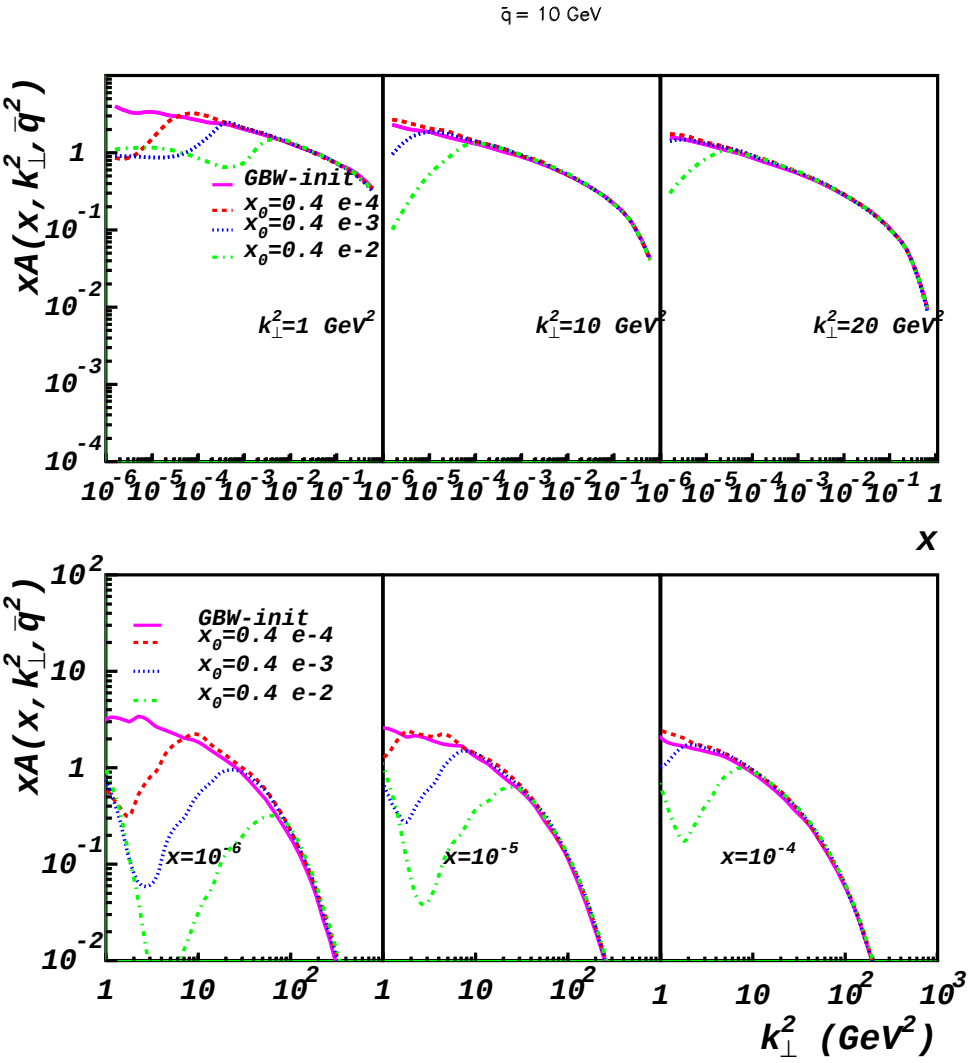

Figure 6: *Unintegrated CCFM gluon density as a function of x for different values of $k_\perp$ at $\bar{q} = 10$ GeV. Different values of the saturation scale Q_s are used, indicated by the differetn values of x_0.*

4 Processes for determination of uPDF

Constraints on the unintegrated parton densities can be obtained from any process, where information on the energy and the transverse momentum of the incoming parton can be obtained (see Fig. 7). Such processes can be multi - jet production in DIS and heavy flavor production (charm) in photoproduction and DIS. The idea in both cases is to identify the hard interaction closest (in ra-

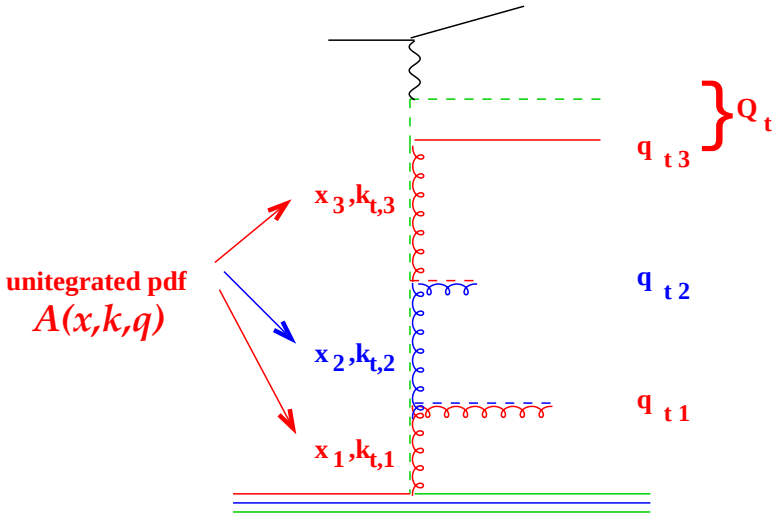

Figure 7: *Schematic diagram for constraining the unintegrated gluon distribution.*

pidity) to the photon via a dijet system with a certain $p_\perp$or via tagging charm (either single or double tag). Then those jets (from the inclusive $k_\perp$algorithm) are analyses, which are farer and farer away (in rapidity) from the photon. By successively reconstruction of x_g and $k_\perp$, the unintegrated gluon density can be obtained as a function of the rapidity, or equivalently $\bar{q}$. Important is, that the jets are ordered in rapidity.

4.0.3 Multi-jet Production

1. dijet production in DIS
   Measure x_g and $k_\perp$ or plot S versus x_g

2. dijet production in γp

3. dijet production in DIS
   Measure x_g and $k_\perp$ or plot S versus x_g

4. 3-jets scenario
   measure α_s from 2 to 3 jet ratio
   multiple scatterings
   correlations in $\gamma p \to 2, 3$jets at small $p_\perp$
   ϕ correlations
   $p_\perp$ correlations

5. Multi jet and mini jet production in DIS
   Measure x_g and $k_\perp$ as function of η in dijet, 3jet, 4jet production
   investigation of fwd region (Calo and tracking)
   use tracker for jets, fwd tracker also ????
   include diffraction
   separate multiple scattering regions:
   jet profiles for small x and large x_γ (or as a fct of η)
   understand parton cascades
   improve jet reco: det-had corrections for small $p_\perp$ jets
   fwdjet + 1,2,3,.. jets
   $p_\perp$, η spectra
   correlations
   similar to Tevatron analysis
   look on away side energy flow ($60 < \phi < 120$, from jet) as fct of jet-$p_\perp$

6. prompt photons
   Et flow away from jets/photon
   xsect for $\gamma + 1$ jet
   $\gamma + 2$ jet
   $\gamma + 3$ jet
   $\gamma + 4$ jet
   .... measure α_s from 1 to 2 jet ratio
   un-integrate quark density
   multiple scatterings
   diffraction

4.0.4 Heavy Flavor Production

1. single tag in γp + n-jet
   D^* + jet: 1,2,3 etc jets. continue Geros analysis
   measure α_s from D^* +1 jets to D^* + 2 jet
   include fwd region
   reconst. 4 jets (incl. c-jets)
   measure contribution of quark initiated charm production
   integrated gluon D^* + jets
   measure unintegrated quark density including diffraction
   look at Et flow opposite to charm, and in $60 < \phi < 120$ as fct of $p_\perp$

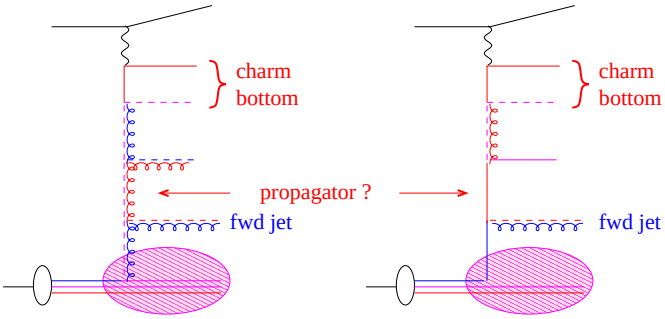

compare to jets

2. single tag in $\gamma p + fwd$-jet
   measure x_{jet} and $p_{T\,jet}$ x-section. Is D^* + fwd jet also $\sim 1\%$ of $\sigma(D^*)$
   measure σ vrs $W_{\gamma p}$
   fwd jets with charm quarks in central region
   $\rightarrow$ much smaller xgluon accessible
   fwd jets with strange tag (K_0/Λ)

3. single tag in $\gamma p + fwd$-π
   measure as above...

4. charm and strange
   D^* plus K_0/Λ
   compare to jets + K_0/Λ
   investigate string structure of strangeness production
   strange particle production: (continue + extend C Risler analysis)
   comparison diffraction/non-diffraction
   eliminate p-remnant contribution

5. double tag in γp + jet
   reconstruct x_g, reconstruct $\bar{q} = x_g\sqrt{s\Xi}$ with $\Xi = \exp(-2\eta^{c\bar{c}})$ in ep cms
   measure $k_\perp = p^c_\perp + p^{\bar{c}}_\perp - p^\gamma_\perp$

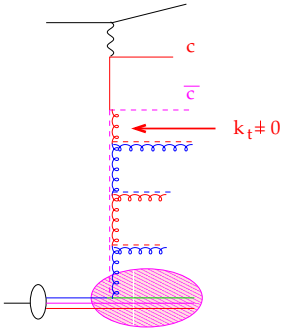

6. double tag in γp and γp + n-jet
   n = 0, 1,2,3 etc jets, continue Jeannine

reconstruct x_g, reconstruct $\bar{q} = x_g\sqrt{s\Xi}$ with $\Xi = \exp(-2\eta^{c\bar{c}})$ in ep cms
measure $S(x, Q^2, \Delta\Phi) = \frac{\int_0^{120^o} d\sigma d\Phi}{\int_0^{180^o} d\sigma d\Phi}$
improve ϕ correlations
include jets for ϕ correlations
unintegrated gluon

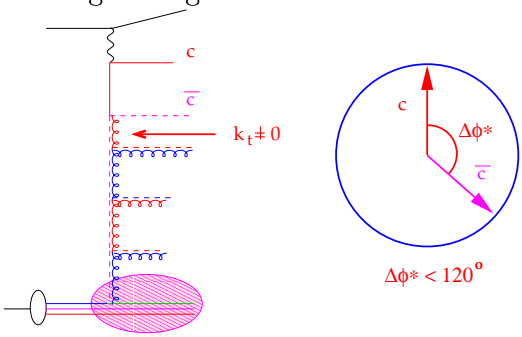

7. double tag in $\gamma p + fwd$-jet
identify both charm quarks, measure $\Delta\eta^{c\bar{c}}$
small $\Delta\eta^{c\bar{c}} \rightarrow$ small x_g
measure $\Delta\eta^{c\bar{c},jet} = \eta^{c\bar{c}} - \eta_{fwd\,jet}$
small $\Delta\eta^{c\bar{c}} \rightarrow$ large $\Delta\eta^{c\bar{c},jet}$

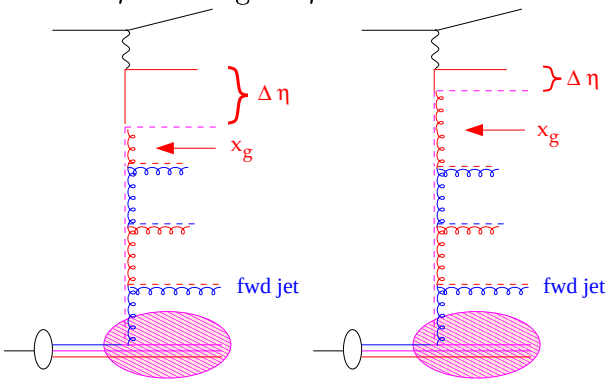

8. charm: semi-inclusive + jets
$\cos(\theta^*)$ distributions
investigate propagator effects in parton cascade (extending ZEUS analysis)
investigate unintegrated quark density

4.0.5 Tools and MC development

1. MC development - CASCADE
include quarks include multiple scatterings (standard) unintegrated gluons/quarks global fits

2. CASCADE and multiple scatterings (collaboration with J. Bartels)
   include multiple scatterings
   → solve saturation problem
   → solve connection diffraction-non-diffraction
   transport experience from mult.scattering at HERA to LHC

3. CASCADE and parton density evolution (collaboration with S. Jadach)
   develop and include fwd parton evolution
   perform global fits to F_2 and had final state and heavy quarks
   extension to LHC

5 Description of the Program

All the above described analyses should aim at a fit of the parton distribution functions. In the first round, no attempt will be done to extract the parton distribution function, but the input parameters of the parton distribution functions should be adjusted (fitted) such that the measured visible cross section can be described with:

1. DGLAP based hadron level Monte Carlo (according to Collins scheme), including parton showering and parton evolution
2. DGLAP NLO calculation including parton evolution (probably CTEQ program, or Botje program, or Pascaud program)
3. DGLAP (one loop) evolution of uPDF using CASCADE or similar in collaboration with Cracow theory (W. Broniowski, A. Szczurek)
4. CCFM (all loop) evolution of uPDF using CASCADE or similar in collaboration with Cracow theory (W. Broniowski, A. Szczurek)

The next step involves including as an additional constraint $F_2(x, Q^2)$ in the above fitting procedure, with the aim obtaining an *H1 global fit* of parton distribution functions. In all the above, α_s will be fixed to the world average.

In a 3rd step, the above fits will be repeated, including the $F_2(x, Q^2)$ constraints, with also fitting α_s.

The final aim is to obtain parton distribution function from a global H1 fit, with error estimate, which describes best inclusive and exclusive measurements, or in the worst case, provide different set of pdfs and uPDF's, which can be used in different regions of phase space.

In a 4th step, the above can be repeated to obtain the double uPDF's as advertised by the Durham group.

6 Diffraction

A deeper understanding of diffraction and its connection to standard processes is still lacking. By measuring heavy quark events accompanied with a forward jet, as described above, together with the observation of a gap in rapidity without particle production in a region close to the proton remnant system (diffractive selection), a new class of events can be selected, which has never been observed and studied before. This process could yield direct information about the contribution of multiple gluon exchange (in addition to the one-parton exchange in standard processes) mechanisms to the forward jet cross section, which already shows large deviations from standard theoretical predictions. Thus this study could serve as a tool of understanding diffraction in terms of a perturbative 2-gluon exchange mechanism and to understand the transition from diffractive to non-diffractive processes.

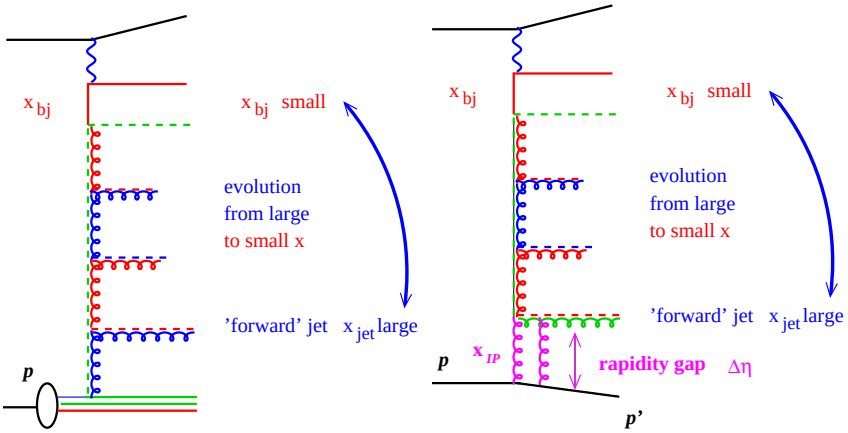

The same measurements and analyses as described above for the non-diffractive case should be performed also for diffraction.

1. rapidity gap method
2. VFPS

The emphasis should be on a deeper understanding of saturation effects, the small $k_\perp$region of the uPDF will be very interesting. Investigating the jet production as a function of rapidity, a direct comparison with non-diffraction should be possible: in the region far away (in rapidity) from the rapidity gap, diffractive and non-diffractive should be similar, if the same hard subprocess are involved, based on single parton exchange. If however multiple parton exchange plays a significant role, as suggested by the perturbative 2-gluon calculations [31], then even there a difference should be observable.

Moving closer and closer (in rapidity) to the rapidity gap, the difference of the uPDF of diffraction and non-diffraction should become more and more

visible, at the end showing a clear sign of multi-parton exchange (which could be interesting also for multiple scattering processes in non-diffractive processes).

References

[1] V. Gribov, L. Lipatov, *Sov. J. Nucl. Phys.* **15** (1972) 438 and 675.

[2] L. Lipatov, *Sov. J. Nucl. Phys.* **20** (1975) 94.

[3] G. Altarelli, G. Parisi, *Nucl. Phys.* **B 126** (1977) 298.

[4] Y. Dokshitser, *Sov. Phys. JETP* **46** (1977) 641.

[5] E. Kuraev, L. Lipatov, V. Fadin, *Sov. Phys. JETP* **44** (1976) 443.

[6] E. Kuraev, L. Lipatov, V. Fadin, *Sov. Phys. JETP* **45** (1977) 199.

[7] Y. Balitskii, L. Lipatov, *Sov. J. Nucl. Phys.* **28** (1978) 822.

[8] S. Catani, M. Ciafaloni, F. Hautmann, *Nucl. Phys.* **B 366** (1991) 135.

[9] J. Collins, R. Ellis, *Nucl. Phys.* **B 360** (1991) 3.

[10] L. Gribov, E. Levin, M. Ryskin, *Phys. Rep.* **100** (1983) 1.

[11] E. M. Levin, M. G. Ryskin, Y. M. Shabelski, A. G. Shuvaev, *Sov. J. Nucl. Phys.* **53** (1991) 657.

[12] M. Ciafaloni, *Nucl. Phys.* **B 296** (1988) 49.

[13] S. Catani, F. Fiorani, G. Marchesini, *Phys. Lett.* **B 234** (1990) 339.

[14] S. Catani, F. Fiorani, G. Marchesini, *Nucl. Phys.* **B 336** (1990) 18.

[15] G. Marchesini, *Nucl. Phys.* **B 445** (1995) 49.

[16] J. R. Forshaw, A. Sabio Vera, *Phys. Lett.* **B440** (1998) 141.

[17] B. R. Webber, *Phys. Lett.* **B444** (1998) 81.

[18] G. Salam, *JHEP* **03** (1999) 009.

[19] J. C. Collins, X.-M. Zu, *JHEP* **06** (2002) 018.

[20] S. Catani, Aspects of QCD, from the Tevatron to LHC, in *Proceedings of the International Workshop* Physics at TeV Colliders (Les Houches, France, 8-18 June, 1999), hep-ph/0005233.

[21] G. Bozzi, S. Catani, D. de Florian, M. Grazzini, *Phys. Lett.* **B564** (2003) 65.

[22] A. Kulesza, W. J. Stirling, *JHEP* **12** (2003) 056.

[23] S. Catani, D. de Florian, M. Grazzini, P. Nason, *JHEP* **07** (2003) 028.

[24] H. Jung, *Mod. Phys. Lett.* **A19** (2004) 1, hep-ph/0311249.

[25] A. Gawron, J. Kwiecinski, Resummation effects in Higgs boson transverse momentum distribution within the framework of unintegrated parton distributions, 2003, hep-ph/0309303.

[26] A. Gawron, J. Kwiecinski, W. Broniowski, *Phys. Rev.* **D68** (2003) 054001.

[27] G. Watt, Unintegrated partons to describe the P(T) distribution of W and Z bosons at the Tevatron, hep-ph/0309096.

[28] G. Bottazzi, G. Marchesini, G. Salam, M. Scorletti, *JHEP* **12** (1998) 011, hep-ph/9810546.

[29] J. Kwiecinski, A. Martin, P. Sutton, *Phys. Rev.* **D 52** (1995) 1445.

[30] R.K. Ellis, W.J. Stirling, B.R. Webber, *QCD and collider physics* (Cambridge University Press, 1996).

[31] J. Bartels, H. Jung, M. Wusthoff, *Eur. Phys. J.* **C 11** (1999) 111, hep-ph/9903265.